No alloying in Fe deposited on Pd(001) at room temperature

H. L. Meyerheim,* R. Popescu, and J. Kirschner
Max-Planck-Institut für Mikrostrukturphysik, Weinberg 2, D-06120 Halle, Germany
(Received 23 August 2005; revised manuscript received 2 May 2006; published 27 June 2006)

Using surface x-ray diffraction we have investigated growth and structure of Fe deposited on Pd(001) at room temperature. Up to about 4.2 ML, the maximum film thickness studied, Fe grows in layer-by-layer mode without sizable intermixing with Pd. Up to 1.5 ML coverage the Fe film adopts a fct-structure followed by a transition to a bct-structure at higher film thickness. The top Pd interlayer spacing, which in the case of uncovered Pd(001) is expanded by up to $6.5\pm2.0\%$ relative to the bulk due to adsorbed hydrogen relaxes to $0\pm2\%$ upon adsorption of 0.6 ML Fe, possibly due to displacement into subsurface sites. Mild annealing (400 K) of a 1 ML Fe/Pd(001) sample induces surface alloying leading to a disordered two layer thick fct-$Fe_{50}Pd_{50}$-alloy.

DOI: 10.1103/PhysRevB.73.245432 PACS number(s): 68.35.Ct, 61.10.−i, 75.70.Ak

I. INTRODUCTION

The interest in Fe-Pd systems goes back several decades since it was discovered that Pd acquires a magnetic moment in the presence of magnetic impurities in the bulk.[1–3] More recently, it has been found that *ordered* FePd alloys exhibit perpendicular magnetic anisotropy (PMA), which is an important property for technological applications in high density magnetic storage applications.[4–7] Thus, intense efforts to characterize the growth, structure, and magnetic properties of Fe on Pd(001) and related alloys were made, but a clear picture has not evolved yet.

In 1990, Liu and Bader[8] as well as a decade later Jin *et al.*,[9] using scanning tunneling microscopy (STM) and reflection high energy electron diffraction (RHEED), determined layer-by-layer growth mode of Fe on Pd(001). In contrast, Quinn *et al.*[10] did not find clear evidence for layer-by-layer growth.

With regard to the interface structure some controversy also exists. More recent studies using low energy electron diffraction (LEED)[11] and surface x-ray extended absorption fine structure measurements[12] found evidence for substantial surface alloying for a 4-ML-thick film, while earlier studies, albeit less focused on the detailed interface structure,[10,13] did not determine alloy formation. Here and in the following we refer to an Fe coverage (Θ_{Fe}) of 1 ML as one adatom per substrate atom, i.e., 1.32×10^{15} atoms/cm^2. Surface alloy formation is likely to occur, since Fe and Pd are miscible in the bulk and several stable ordered bulk phases exist, such as FePd and $FePd_3$, both ordering ferromagnetically.[14,15]

The magnetic properties of FePd alloys were correlated with their structure. Formation of a (disordered) face centered tetragonal (fct) FePd surface alloy was related to the strong magnetic in-plane anisotropy found for room temperature (RT) deposited films.[4,12] In contrast, an ordered FePd alloy was proposed to exhibit PMA. PMA was also observed in experiments where epitaxial Fe layers were deposited on Pd(001) at 100 K up to a thickness of 2.5 ML.[8] This was attributed to an abrupt interface, since at this low temperature, alloying is believed to be suppressed.

In order to elucidate in detail the Fe/Pd(001) interface formation, we have carried out a systematic surface x-ray diffraction (SXRD) study. Clear evidence is presented that there is *no alloying* for Fe deposition at RT, while interface alloying sets in at low annealing temperature ($\approx$330 K). Fe adsorption also significantly affects the top Pd-interlayer distances, d_{12} and d_{23}. This is tentatively attributed to the displacement of surface adsorbed hydrogen, possibly into subsurface sites.

II. EXPERIMENT

The experiments were carried out in an ultrahigh vacuum system using a z-axis diffractometer setup for the SXRD data collection.[16] The Pd(001) crystal was cleaned by standard methods (Ar^+-ion sputtering followed by annealing at 900 K) until no traces of contaminants could be observed by Auger-electron spectroscopy (AES). In all cases it was ensured that before Fe deposition the sample was cooled to 300 K after annealing. Fe was deposited by evaporation from an Fe rod heated by electron bombardment.

The amount of Fe deposited was calibrated by AES and *a posteriori* compared with the SXRD-derived coverage. In general, good agreement between the so derived Fe coverages within the error bars of about 0.2 ML was determined.

X rays were generated by a rotating anode system and monochromatized (Cu-Kα radiation) by using a focusing graphite monochromator yielding a peak count rate of several hundred cts./s at the (1 0 0.05) reflection. This position is close to the (100) anti-phase condition along the (10ℓ) crystal truncation rods (CTR).[17–19] The CTRs arise from the truncation of the crystal, therefore the coordinate ℓ of the normal momentum transfer $q_z=\ell\times c^\star$ becomes a continuous parameter ($c^\star=1.61$ Å^{-1} is the reciprocal lattice unit of Pd along q_z).[20] The detailed calculation shows that at the (100) position the scattered intensity of the whole (semi-infinite) crystal is proportional to a quarter of a Pd monolayer, i.e., $I(100)\propto(f_{Ag})^2/4$, where f_{Ag} is the atomic scattering factor of Ag.

Integrated x-ray reflection intensities were collected under total reflection conditions of the incoming beam (incidence angle $\alpha_i\approx0.32°$) by rotating the sample about its surface normal.[18,19] In total, 13 data sets were collected, three for the clean sample and ten for the Fe covered Pd(001) surface in

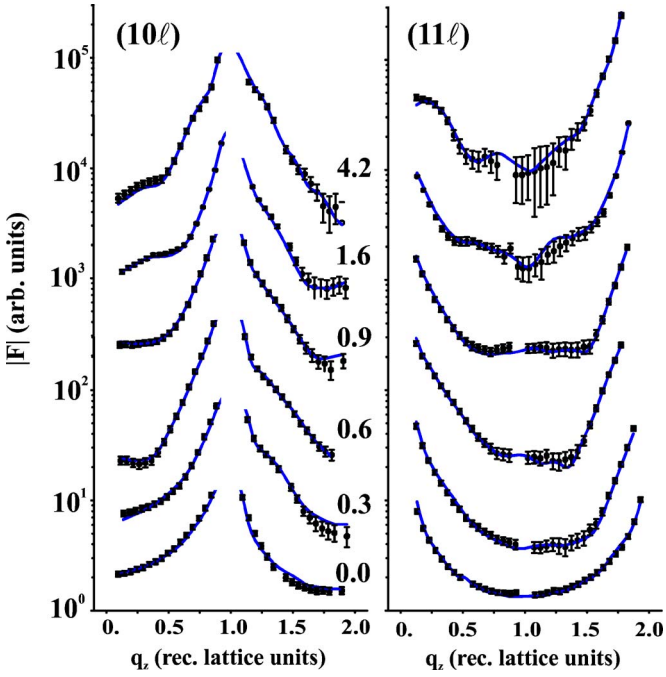

FIG. 1. (Color online) Measured (symbols) and calculated (lines) structure factor amplitudes $|F|$ along the (10ℓ) (left) and the (11ℓ) (right) CTR for clean (0.0 ML) Pd(001) and after deposition of 0.3, 0.6, 0.9, 1.6, and 4.2 ML Fe (from bottom to top). Curves are successively shifted by about half an order of magnitude.

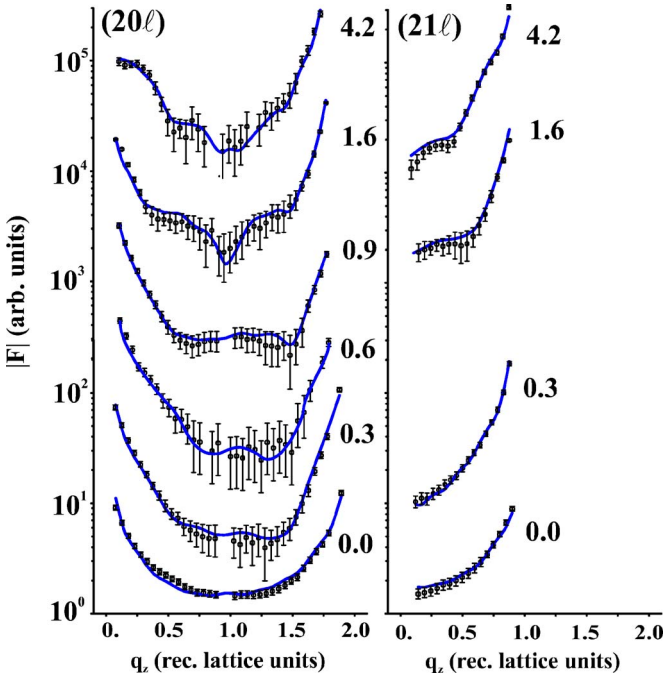

FIG. 2. (Color online) Measured (symbols) and calculated (lines) structure factor amplitudes $|F|$ along the (20ℓ) (left) and the (21ℓ) (right) CTR for clean (0.0 ML) Pd(001) and after deposition of 0.3, 0.6, 0.9, 1.6, and 4.2 ML Fe (from bottom to top). Curves are successively shifted by about half an order of magnitude.

the coverage range between 0.1 and 4.2 ML. In addition, one data set was measured after annealing a 1 ML sample at 400 K for 10 min.

For each data set (deposition) in general four symmetry *independent* CTRs [(10ℓ), (11ℓ), (20ℓ) and (21ℓ)][17] were collected corresponding to about 120 independent reflections. In order to estimate the contribution of systematic errors to the total standard deviation (σ) of each reflection, the $|F|$'s of one symmetry equivalent rod [e.g. (01ℓ) according to the $p4mm$ plane group symmetry] were collected. The reproducibility was in the range of several percent, which—apart from some very weak reflections, where the statistical error is dominant—represents the σ's of the $|F|$'s in general (for details see Refs. 18 and 19). In total, the collection of a full data set took up to 48 h. AES measurements carried out after the SXRD measurements indicated in two cases trace amounts of oxygen contaminations. However, based on the repeated measurements of x-ray control reflections during data collection, these contaminations seem not to affect the structure of the Fe/Pd(001) interface, since time dependent changes of reflection intensities were not detected.

Symbols in Figs. 1 and 2 represent the structure factor amplitudes $|F|$ along the (10ℓ) and the (11ℓ) CTR as well as for the (20ℓ) and the (21ℓ) CTR collected for the uncovered sample and after deposition of 0.3, 0.6, 0.9, 1.6, and 4.2 ML Fe (from bottom to top as indicated in the figure). Curves are successively shifted for clarity. Standard deviations (σ) are indicated by the error bars. The $|F|$'s were derived from the integrated intensities after correction for geometric factors.[21]

The (21ℓ) CTR was measured up to $\ell=0.85$, which for the given wavelength (1.541 Å) is close to the experimental limit imposed by mechanical constraints. In the presented selection of the data, the (21ℓ) rod was not measured for the 0.6 and 0.9 ML sample, however without any sizable effect on the fit convergence and on the accuracy of the refined parameters.

Direct inspection of the rods already allows some qualitative conclusions, which are verified by fitting the intensities along the rods (see below). First, there is an equivalence of the overall shape between the (11ℓ) and the (20ℓ) as well as between the (10ℓ) and (21ℓ)-CTRs. Some difference between the absolute intensities is due to the decrease of the atomic scattering amplitudes with increasing scattering vector and the effect of disorder. The apparent "equivalence" is related to the occupation of high symmetry in-plane sites by Fe and Pd atoms in the $p4mm$ plane group. These are fixed either at (0.,0.) or $(1/2,1/2)$, alternating layer by layer. For the corresponding CTR pairs this means that the in-plane phase factor, $\exp[i2\pi(hx+ky)]$ is identical. With regard to the data analysis this is quite a favorable situation, since this reduces the number of refinement parameters considerably as will be discussed in more detail below.

Second, while for the uncovered Pd(001) surface the intensity distribution along the CTRs is characterized by the U-shaped profiles (on log scale), adsorption of Fe significantly changes the rod profiles. In the low coverage regime, up to about 0.9 ML, the intensity distribution along the rods is steeper as compared to that of the uncovered sample. Qualitatively this can be interpreted by Fe adsorption in hollow sites. For this particular case the scattered intensity at the (100)-(anti-phase) reflection position is given by: $I(100) \propto |f_{\mathrm{Pd}}/2\text{-}\Theta_{\mathrm{Fe}} \times f_{\mathrm{Fe}}|^2$, where the f's and Θ_{Fe} represent the

atomic scattering factors and the Fe coverage in ML. Consequently, with increasing Θ_{Fe} the intensity at the anti-phase condition is reduced, while there is (always) negligible change close to the in-phase (bulk-Bragg) condition. In consequence this leads to an increased intensity dynamics along the CTR. At higher coverages the situation changes due to second layer Fe adsorption and the intensity variation becomes more oscillatory.

The quantitative structure analysis was carried out by least square refinement of the calculated $|F|$'s to the experimental ones. As a consequence of the *p4mm* plane group symmetry and the simple body centered tetragonal structure there is only one independent atomic in-plane position per layer located either at (0,0) or $(\frac{1}{2},\frac{1}{2})$, within the (primitive) two-dimensional unit cell. Therefore, apart from an overall scale factor only one z parameter and one Debye parameter (B) representing (isotropic) disorder[22] needs to be refined for each layer. The parameter B is related to the mean square displacement of the atoms out of their equilibrium position, $\langle u^2\rangle$, by the relation: $B=8\pi^2\langle u^2\rangle$. Throughout the samples we determine maximum values up to about 3 Å^2, corresponding to root-mean square (rms) displacements ($\sqrt{\langle u^2\rangle}$) of 0.18 Å. In comparison with bulk (thermal) disorder ($\sqrt{\langle u^2\rangle} \approx 0.10$ Å) this indicates a significant enhancement, commonly observed for surfaces. In addition to the Fe adlayers, several Pd substrate layers were included in the analysis until convergence of the fit quality was achieved. Possible alloying can be taken into account by fractional occupancy factors ($\Theta_{Fe,Pd} \leqslant 1$) for a given position.

In all cases very good fits as represented by the solid lines in Figs. 1 and 2, could be achieved. The fit quality is measured by the un-weighted residuum (R_u), which is the average relative deviation between the experimental and calculated $|F|$'s.[23] Following a recommendation of the International Union of Crystallography, in addition to R_u we use the goodness of fit (GOF) parameter as a global measure of the fit quality.[24] It is defined as: GOF $=\sqrt{\frac{1}{N-P}\Sigma w(|F_{obs}|-|F_{calc}|)^2}$, where N and P are the number of reflections and refined parameters, respectively, and $w=1/\sigma^2$ is the weighting factor using the standard deviation (σ) as parameter.[25] The summation runs over all data points. Thus, the GOF takes into account the difference between the number of data points and the number of free parameters. GOF should be close to unity if the weights of the observations have been correctly assessed. In the present study there is a large over determination of the refinement problem, since per layer only two parameters, namely one z coordinate and one B factor needs to be refined, adding to typical $P=10$ parameters only. This is quite a low number as compared to the $N=120$ data points the average data set consists of (see above).

In addition, it is important to mention that for the least squares fit, the correlation (C) between the parameters is also decisive. A high number of large correlations (e.g., $|C|>0.8$) between parameters can severely affect the fit convergence, its quality, and the standard deviations of the parameters (σ_P) as derived from the variance-covariance matrix.[26] In this study as well as in a number of other ones concerned with interface structures on high-symmetry substrate surfaces (see, e.g., Refs. 27 and 28), we are in the favorable situation that the parameter correlations were quite low ($|C|<0.6$) with only a few above this value leading to rapid fit convergence and small standard deviations of the fit parameters.

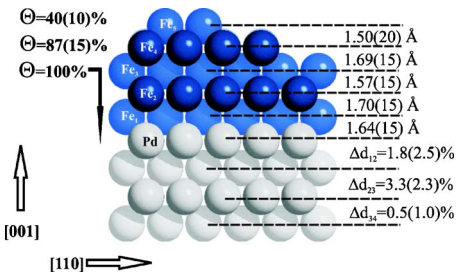

FIG. 3. (Color online) SXRD derived structure model for 4.2 ML Fe/Pd(001). Blue (dark) and gray (bright) balls represent Fe and Pd atoms, respectively. Adlayer distances in Å and deviations of the substrate layer spacings relative to bulk Pd are listed on the right. Number in brackets indicate error bars. Labels Fe_1 to Fe_5 indicate the Fe layers from bottom to top.

As shown in Ref. 27 as well as in this study, the σ_P's derived from the variance-covariance matrix seem to overestimate the error bars of the z-coordinate determination when compared with the reproducibility of the results derived from independent experiments. Nevertheless, we use the σ_P's from the fit, since these are based on a reproducible and well established procedure. Throughout this study, for the best fit models **excellent** residuals were achieved. In detail, for the GOFs we obtain: 0.0 ML:1.3; 0.3 ML:0.8; 0.6 ML:1.1; 0.9 ML:0.8; 1.6 ML:1.0; 4.2 ML:1.0. Similarly, R_u is in the range between 0.04 and 0.07. Trying different models (e.g., an alloy model for the nonalloyed as deposited Fe/Pd(001) interface or vice versa), leads to residuals larger by a factor of at least 3, allowing clear and unambiguous analysis of the structures as will be outlined in the following.

III. RESULTS OF THE STRUCTURE ANALYSIS

A. Fe/Pd(001)

In the first part of the analysis we concentrate on Fe/Pd(001) prepared at substrate room temperature. The structure of annealed Fe/Pd(001) will be discussed in Sec. III B. From the data analysis several results were obtained:

(i): Within an uncertainty of about 10%–15% for the determination of the (layer resolved) layer occupancy, there is no Fe/Pd interface mixing. Fe grows epitaxially on the Pd(001) surface. A model for the 4.2 ML Fe/Pd(001) sample is displayed in Fig. 3 in side view. Blue (dark) and gray (bright) balls represent Fe and Pd atoms, respectively. Interlayer distances given in Å and changes of substrate layer spacings (relative to the bulk spacing of 1.945 Å) are indicated on the right. Occupation factors for the topmost incomplete Fe layers are indicated on the left hand side.

Our result of negligible intermixing is at some variance with previous studies.[11,12] We relate this to slight differences in the sample preparation. For example, in their quantitative intensity versus energy (IV) LEED analysis, Lee *et al.* deter-

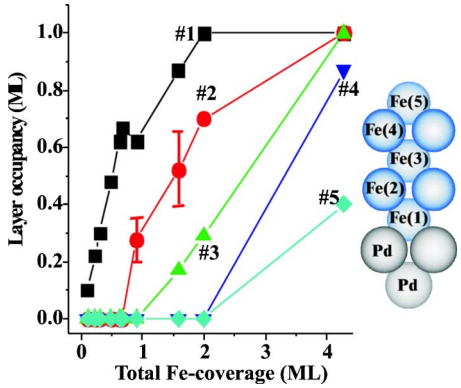

FIG. 4. (Color online) Layer resolved occupancy vs total Fe coverage. Numbers label the Fe layers from 1 (bottom, next to the interface) to 5 as shown schematically in the schematic structure model on the right. Error bars are in the ±0.15 range. Lines are guides to the eye.

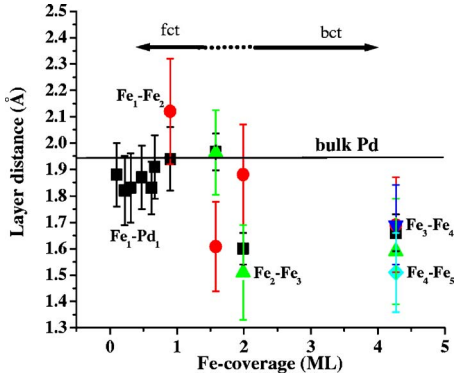

FIG. 5. (Color online) Layer spacings in Fe/Pd(001). Labels Fe_i-Fe_j or Fe_i-Pd_j indicate interlayer distances between corresponding layers as shown in the schematic structure model in Fig. 4. The horizontal solid line represents the bulk Pd-layer spacing. The fct- and bct-Fe structure regimes are indicated by the arrows.

mine substantial alloying for 1 and 2 ML Fe deposited on Pd(001). Notably, the authors report that the substrate temperature during deposition was around 320–330 K, i.e., well above 300 K, which was used in our experiments. As will be discussed in more detail in Sec. III B, we find that interface mixing already starts in the temperature range of 330 K.

Similarly, no alloy formation for Co deposited at room temperature on Pd(001) was found also in a recent SXRD study.[28] In this study it could be shown that alloying is only observed for pulsed laser deposited Co, where due to the high energy of the arriving atoms of the order of several eV[30] the activation energy (0.5 eV[28,29]) for the site exchange process can be overcome. In contrast, the kinetic energy for thermally deposited atoms (e.g., 300 K≅25 meV) is not sufficient to overcome the activation barrier for intermixing.

(ii): Up to the maximum coverage investigated (4.2 ML), the Fe film grows in a layer-by-layer like mode in agreement with the RHEED and scanning tunneling microscopy (STM) study of Jin *et al.*[9] As an example, for the 4.2 ML sample, five Fe layers are identified, three complete ones ($\Theta_{Fe}=1.0$), and two incomplete ones at the top of the film. These are filled by 87±15% and 40±10%, respectively.

Figure 4 shows the layer resolved Fe occupancy versus total Fe coverage for all ten samples. Different symbols correspond to different Fe layers as indicated by the labels 1 (first layer next to the Pd substrate) to 5 (topmost layer). The beginning of second layer growth is first observed for 0.9 ML. The third layer first appears at about 1.5 ML, where the first and second layer are filled to about 80% and 50%, respectively. Comparison with the STM images of Jin *et al.*[9] yields good agreement in general. There is only one slight disagreement for the coverage 1.6 ML (Jin *et al.* 1.4 ML), where the STM images do not show islands of the third layer, while the SXRD data indicate the presence of some fraction (≈17%) of third layer Fe. This disagreement might be attributed to the different Fe coverages of the samples, since for all other cases, where the Fe coverage is identical, the correspondence between STM and SXRD is satisfying. For example, the STM image for 1.9 ML shows a 10% fraction of third layer islands (SXRD: 29±15) above an almost complete (85%, SXRD: 70±15) second layer.

(iii): We have some evidence for a transition from fct-Fe to body centered tetragonal (bct)-Fe taking place in the coverage regime between about 1.5 and 2 ML. Figure 5 summarizes all adlayer distances versus Fe coverage. Solid squares represent the Fe-Pd spacing at the interface. The interlayer distances between the following Fe adlayers are represented by filled circles (Fe_1-Fe_2), up triangles (Fe_2-Fe_3), down triangles (Fe_3-Fe_4), and diamonds (Fe_4-Fe_5). The labeling of the Fe layers refers to Fig. 3. Error bars represent standard deviations as derived from the variance-covariance matrix.

Although in some cases the error bars are quite large due to the low scattering contribution of incompletely filled layers, in general two regimes can be distinguished: the first in the range $0<\Theta_{Fe}\leqslant 1.5$ ML characterized by interlayer spacings in the range of bulk Pd (1.945 Å), the second for $\Theta_{Fe}>2$ ML characterized by low distances in the range of 1.60 Å.

As pointed out by Quinn *et al.*[10] Fe-interlayer distances in the 1.5–1.6 Å range are related to a distorted bcc Fe-equilibrium structure rather than to a distorted fcc structure. Consequently, the Fe-adlayer structure in the second regime is bct, while in the first regime the film is fct like.

So far it has been argued that interface alloying for RT deposited Fe is related to the experimentally observed in-plane easy magnetization axis.[11,12] Some indirect support for this conclusion came from the study of Liu and Bader[8] where films deposited at 100 K showed an out-of-plane easy axis. It was assumed that at this temperature intermixing is inhibited, while at 300 K surface alloying takes place.

In the context with the theoretical study of Szunyogh *et al.*[4] our result might be interpreted that interface alloying needs not to be invoked to explain in-plane magnetization. In their investigation an in-plane easy axis was determined for Fe on Pd(001), where the Fe layers adopt a fcc geometry with the Pd-bulk lattice constant, very close to the SXRD result for Fe coverages below 1.5 ML. In more detail it was shown that while up to about 3 ML the band energy contribution (E_b) favors an out-of-plane magnetization, the strongly negative dipole energy (E_{dd}) always turns the total

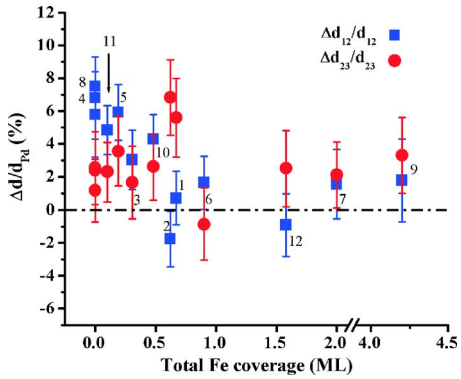

FIG. 6. (Color online) Coverage dependent changes of the Pd-interlayer spacings Δd_{12} and Δd_{23} relative to the Pd-bulk spacing (d_{Pd}). Labels 1–12 indicate data collection sequence.

anisotropy energy (E_a) negative, corresponding to an in-plane magnetization.

(iv): The substrate interlayer distances were also determined. Figure 6 shows the coverage dependent differences of the first ($\Delta d_{12}/d_{\mathrm{Pd}}$, squares) and second ($\Delta d_{23}/d_{\mathrm{Pd}}$, circles) Pd-layer spacings relative to the Pd-bulk spacing (d_{Pd}). Note that all 13 datapoints represent independent measurements. In all cases a new preparation including sample cleaning was carried out. It is also important to mention that the individual data sets were not collected in a definite sequence, e.g., with increasing or decreasing coverage, but in an arbitrary way as follows: 0.67, 0.62, 0.30, 0.00, 0.22, 0.90, 1.99, 0.00, 4.27, 0.475, 0.10, 1.58 ML. This excludes that the results obtained might be biased by an "aging" of the sample, e.g., by alloying or accumulating contaminations. Numbers 1–12 in Fig. 6 represent the sequence of the data collection. Another data set for the uncovered sample (0.00 ML) was taken earlier and a detailed analysis is published in Ref. 34, where an expansion of $\Delta d_{12}=5.8\pm2.6\%$ was determined. This particular data point is the one not labeled in Fig. 6 at zero Fe coverage.

The most remarkable result is the significant reduction of the 6.5% (error bar about two percentage points as estimated from the scatter of the three data points) expanded top interlayer distance (d_{12}) characteristic for the (Fe) uncovered sample to 0% upon Fe deposition. Already after deposition of about 0.65 ML Fe, the top layer expansion is completely relaxed. Increasing the Fe coverage beyond 0.65 ML has no significant influence on d_{12} anymore. It remains constant and bulk-like within the error bar ($\approx 2\%$).

From previous investigations it is known that hydrogen adsorption induces an expansion of the top Pd-interlayer spacings[31–34] due to the weakening of the Pd-Pd back bonds. In the most recent quantitative LEED and SXRD study[34] a systematic analysis of the Pd top layer expansion was carried out. For Pd(001) covered completely by hydrogen in hollow sites an expansion of $\Delta d_{12}=4.7\pm1.0\%$ was determined. This value is somewhat larger than reported in previous LEED experiments on the "clean" Pd(001) surface [2.5% (Ref. 31), 3% (Ref. 32) and 4.6% (Ref. 33)], but smaller than the average SXRD value of 6.5%. However, a recent theoretical study[35] pointed out that these discrepancies can be related to different hydrogen coverages, depending on the sample preparation. In detail, a linear dependence of Δd_{12} on the hydrogen coverage was predicted with a maximum of $\Delta d_{12}=4.8\%$ for 1 ML hydrogen adsorbed in hollow sites. While this is well in agreement with the LEED result of Refs. 33 and 34 (4.7%) it is by about two percentage points smaller than the value derived by SXRD analysis. An explanation for this discrepancy was also suggested by Jung and Kang,[35] calculating the first two top layer expansions, Δd_{12} and Δd_{23} for 1.25 ML coverage, thereby assuming additional occupation of 0.25 ML hydrogen in octahedral subsurface sites. For this model almost perfect agreement between experiment and theory is obtained ($5.8\pm2.8\%$ vs 5.8% for Δd_{12} and $2.4\pm2.8\%$ vs 2.6% for Δd_{23}), suggesting that in the SXRD experiment the sample is covered by a larger amount of hydrogen than in the LEED experiments. This appears quite reasonable, since both sample preparation and data collections take considerably more time (48 h) to be carried out leaving more time for adsorption of hydrogen from the residual gas atmosphere. For details we refer to Ref. 34.

Since the recent experimental and theoretical studies have given evidence that the top layer expansion is related to hydrogen adsorption, we suggest that the observed "quenching" of Δd_{12} is related to the displacement of surface adsorbed hydrogen upon Fe adsorption. Simultaneously with the relaxation of d_{12} we observe an increase of d_{23}. For the Fe-uncovered sample, d_{23} is expanded by about $2\pm1\%$ on average. In the coverage regime between about 0.5 and 0.7 ML, where d_{12} is relaxed to the bulk value, d_{23} reaches a maximum of about $6\pm2\%$. At larger Fe coverages, d_{23} decreases to about 2%–3%.

This "anomaly" might also be related to hydrogen, which possibly is (partly) incorporated into the Pd crystal when displaced from the surface hollow site. As pointed out by Wilke *et al.*,[36] the octahedral subsurface site is the energetically next favorable site with a binding energy about 0.3 eV less as compared to the hollow site (2.55 vs 2.83 eV). For this reason it seems reasonable to speculate that some hydrogen could be displaced into the subsurface site as indirectly concluded from the coverage dependent behavior of d_{23}.

B. Fe/Pd(001) annealed

In a second set of experiments we have studied the effect of sample annealing on the interface structure. After deposition of 1 ML Fe on the Pd(001) surface at RT, the sample was heated up to 400 K and kept at this temperature for 10 min. During heating, the (1 0 0.05) reflection intensity increased from 120 counts/s (cps) to 310 cps and remained constant. It should also be noted that the intensity started to increase already at a temperature as low as 330 K.

After sample cooling, CTRs were measured as described above. Curves (B) in Fig. 7 show the measured (symbols) and calculated $|F|$'s (blue lines) of the sample along the (10ℓ) and (11ℓ) CTRs. The model based on the best fit ($R_u=0.067$, GOF=1.2) is outlined in Fig. 8, which shows the structure in side view including several unit cells along the [110] direction in order to clarify the disordered structure. Dark (blue) and bright (gray) balls represent Fe and Pd atoms, respectively.

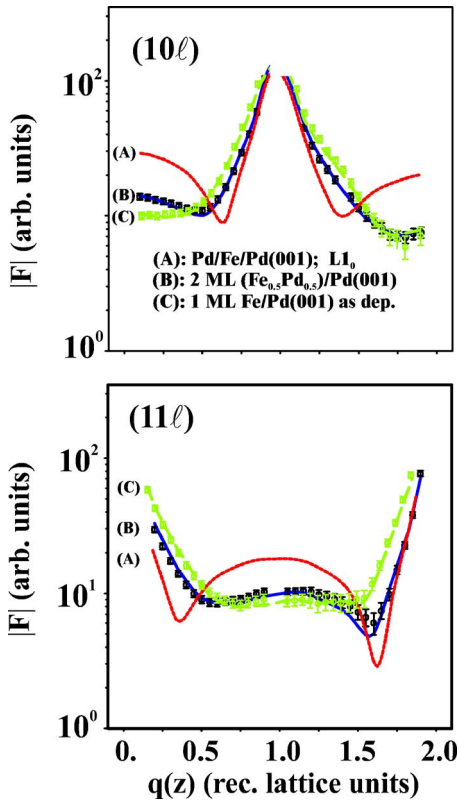

FIG. 7. (Color online) Comparison of experimental (symbols) and calculated (lines) structure factor amplitudes along the (10ℓ) and (11ℓ) CTRs for different samples. The red lines (A) represent the calculated rods for the (ordered) $L1_0$ alloy [Pd/Fe/Pd(001)] interface, (B, blue) and (C, green) show data and best fits for the disordered 2-ML-thick $Fe_{0.5}Pd_{0.5}$ alloy on Pd(001) formed after annealing as deposited 1 ML Fe/Pd(001) (C) at 400 K for 10 minutes. The structure model for (B) is shown in Fig. 8.

We find a two layer $Fe_{0.5}Pd_{0.5}$ *disordered* alloy with a layer spacing of 1.85(10) Å. The spacing to the first pure Pd layer equals 1.93(10) Å. Thus, the structure can be considered as fct like. We have no evidence for any structural ordering as explained in the following. The ordered FePd alloy, which adopts the CuAu-type ($L1_0$) structure, is characterized by a sequence of alternating Fe and Pd layers along the [001] direction. We have calculated the CTRs assuming the layer sequence Pd/Fe/Pd(001), where one ML Fe is embedded

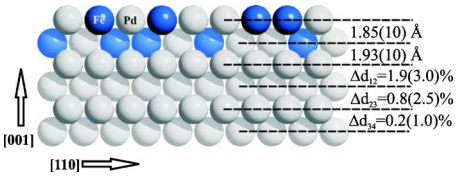

FIG. 8. (Color online) Side view of the structure model derived from SXRD data for 1 ML Fe/Pd(001) annealed for 10 min at 400 K. Bright (gray) and dark (blue) balls represent Pd and Fe atoms, respectively. A (disordered) two layer fct-like $Fe_{0.5}Pd_{0.5}$ alloy forms on Pd(001). Adlayer distances (Å) and substrate relaxations relative to the bulk spacing (1.945 Å) are listed on the right. Numbers in brackets indicate error bars.

between a surface Pd layer and the Pd-bulk crystal corresponding to the (local) $L1_0$ structure. The CTRs are represented in curves (A) as dotted (red) lines. There are strong deviations from the experimental data, characterized by pronounced minima. Qualitatively, the stronger intensity contrast along the rods in the calculation can be explained by the stronger electron density contrast within the sample as compared to that in the actual structure.

The residuals for this model are R_u=0.44 and GOF=6.1, i.e., they are about six times larger than the best fit for the disordered two layer alloy (B, blue line) with R_u=0.067 and GOF=1.1. It should be noted that starting the fit with a model which is that wrong in general leads not only to very large residuals but often to unphysical results (e.g., interatomic distances too short) also.

Apart from the absence of the (local) vertical ordering there is no lateral ordering, since it would lead to superstructure spots, which were not observed.

In the present system involving the atomic species Fe and Pd, the different structure (alloy) models can easily be distinguished from each other. This is because the atomic scattering factors (f) of Fe and Pd differ by about a factor 1.8 ($f \propto Z$, Z=atomic number), therefore the reflection intensities ($I \propto Z^2$) of different structure models are very different. For further comparison, in curves (C, green) of Fig. 7 we have also plotted the experimental (symbols) and calculated (lines) CTRs for the as deposited Fe/Pd(001) interface with a Fe coverage of 0.9±0.1 ML. Also in this case it can be seen immediately that the CTRs for the as deposited sample—characterized by the nonalloy structure—are significantly different from the experimental ones, especially if one takes into account the small standard deviations of the experimental $|F|$'s. In terms of the residuals this is expressed by $R_u \approx 0.30$ and GOF=4.7. Note also that Fig. 7 shows the $|F|$'s (proportional to the square root of the integrated intensities) on a logarithmic scale somewhat obscuring the large differences between the intensities measured for the different structures. The increase of the peak intensity from 120 to 310 cps. at the (1 0 0.05) reflection mentioned above is reflected by the difference between the first points of curves (C) and (B) in the upper part of Fig. 7.

We can compare our model to the LEED-I/V analysis of the 1ML Fe/Pd(001) interface by Lee *et al.*[11] The authors observe alloying with an approximate concentration of $Fe_{0.35}Pd_{0.65}$ and $Fe_{0.90}Pd_{0.10}$ for the first and second layer, respectively (error bars are in the 15% range). This model is different from ours, which is tentatively attributed to the different annealing temperatures (320–330 K deposition temperature in Lee's experiment but annealing at 400 K in ours). In order to explain this difference, one can argue that a higher annealing temperature leads to a structure, which more closely corresponds to a thermodynamic stable phase. For FePd (and CoPd) alloys two such phases exist, namely $Fe_{0.5}Pd_{0.5}$ and $Fe_{0.25}Pd_{0.75}$.[14] It should be noted, however, that the stable FePd phase corresponds to the ordered $L1_0$-type structure, while we find a disordered structure. Formation of the $L1_0$ structure most likely requires higher annealing temperatures, which were not applied in the present set of experiments to avoid extensive alloying of the substrate Pd crystal. Finally, it should be noted that support for this model

comes from our very similar studies on the Co/Pd(001) interface,[28,37] showing the formation of the $L1_0$-alloy structure [Pd/Co/Pd(001)] upon annealing the as-deposited nonalloyed sample to 620 K.

For the interlayer spacings within the alloy, Lee *et al.*[11] find 1.81 Å in perfect agreement with our value but a smaller value for the distance between the second alloy layer to the first Pd layer (1.74 ± 0.02 vs 1.93 ± 0.10 Å). We attribute this to the significantly higher second layer Fe concentration in Lee's sample (90% vs 50% in our case). Assuming that to first order the alloy equilibrium-lattice constant varies linearly with the Fe concentration (Vegard's law), a large concentration of smaller Fe atoms (atomic radii: Pd=1.38 Å, Fe=1.25 Å) involves a larger normal relaxation due to the stronger tensile in-plane strain as compared to alloy layers with a moderate Fe concentration. The validity of this picture has been proven recently in a systematic study on the Pd/Cu(001) alloy formation.[38]

Most remarkably, there is an expansion of the distance between the first pure Pd layers below the alloy: Lee *et al.* find 2.02 ± 0.02 Å in good agreement with the SXRD analysis (1.98 ± 0.05 Å). These values correspond to a 4% and 2% expansion relative to the bulk spacing. Similar expansions were also found for the Co/Pd(001) interface and the pulsed laser deposition grown CoPd alloys.[28,37] As in these cases this is possibly due to hydrogen displaced into the Pd crystal.

IV. SUMMARY

We have presented an *in situ* SXRD analysis of the Fe/Pd(001) interface structure. For thermally deposited Fe on the Pd(001) surface kept at room temperature we find layer-by-layer growth of fct-Fe without sizable (uncertainty $\approx 10\%-20\%$ of a ML) amount of alloying. Discrepancies with previous studies determining interface alloying are attributed to slightly different sample preparation conditions. Above about 2.0 ML, a structural transition from fct to bct-Fe takes place. From the analysis of the top layer spacings of the Pd substrate we tentatively suggest that Fe adsorption induces the displacement of surface adsorbed hydrogen, possibly into subsurface sites. Mild annealing of the as deposited sample (1 ML) up to 400 K leads to the formation of a disordered two-layer-thick fct-like $Fe_{50}Pd_{50}$ alloy.

ACKNOWLEDGMENTS

The authors thank G. Kroder for technical support during the experiments. Helpful discussions with V. Stepanyuk, M. Przybylski, J. Barthel, and X. F. Jin are gratefully acknowledged.

*Electronic address: hmeyerhm@mpi-halle.mpg.de

[1] A. M. Clogston, B. T. Matthias, M. Pettern, H. J. Williams, E. Corenzwit, and R. C. Sherwood, Phys. Rev. **125**, 541 (1962).
[2] G. G. E. Low and T. M. Holden, Proc. Phys. Soc. **89**, 119 (1966).
[3] U. Gradmann and R. Bergholz, Phys. Rev. Lett. **52**, 771 (1984).
[4] L. Szunyogh, J. Zabloudil, A. Vernes, P. Weinberger, B. Ujfalussy, and C. Sommers, Phys. Rev. B **63**, 184408 (2001).
[5] I. Galanakis, S. Ostanin, M. Alouani, H. Dreysse, and J. M. Wills, Phys. Rev. B **61**, 599 (2000).
[6] V. Gehanno, A. Marty, B. Gilles, and Y. Samson, Phys. Rev. B **55**, 12552 (1997).
[7] P. Kamp, A. Marty, B. Gilles, R. Hoffmann, S. Marchesini, M. Belakhovski, C. Boeglin, H. A. Dürr, S. S. Dhesi, G. van der Laan, and A. Rogalev, Phys. Rev. B **59**, 1105 (1999).
[8] C. Liu and S. D. Bader, J. Appl. Phys. **67**, 5758 (1990).
[9] X. F. Jin, J. Barthel, J. Shen, S. S. Manoharan, and J. Kirschner, Phys. Rev. B **60**, 11809 (1999).
[10] J. Quinn, Y. S. Li, H. Li, D. Tian, F. Jona, and P. M. Marcus, Phys. Rev. B **43**, 3959 (1991).
[11] S. K. Lee, J. S. Kim, B. Kim, Y. Cha, W. K. Han, H. G. Min, J. Seo, and S. C. Hong, Phys. Rev. B **65**, 014423 (2001).
[12] C. Boeglin, H. Bulou, J. Hommet, X. Le Cann, H. Magnan, P. Le Fèvre, and D. Chandesris, Phys. Rev. B **60**, 4220 (1999).
[13] V. Cros, F. Petroff, J. Vogel, A. Fontaine, J. L. Menédez, A. Cebollada, W. Grange, J. P. Kappler, M. Finazzi, and N. Brookes, Europhys. Lett. **49**, 807 (2000).
[14] J. J. M. Franse and R. Gersdorf, *Magnetic Propeties of 3d, 4d and 5d Elements, Alloys and Compounds*, Landolt-Börnstein Numerical Data and Functional Relationships in Science and Technology Group III, Vol. 19 (Springer, Berlin 1986).
[15] T. B. Massalski, H. Okamoto, P. R. Subramanian, and L. Kacprack (Eds.) *Binary Alloy Phase Diagrams* (ASM International, Metals Park, OH, 1990), Vol. 20.
[16] M. Bloch, J. Appl. Crystallogr. **18**, 33 (1985).
[17] We use the primitive surface (s) setting of the unit cell, which is related to the face centered setting of the bulk (b) by the following relations: $[100]_s=1/2\times([100]_b-[010]_b)$; $[010]_s=1/2\times([100]_b+[010]_b)$ *and* $[001]_s=[001]_b$.
[18] R. Feidenhans'l, Surf. Sci. Rep. **10**, 105 (1989).
[19] I. K. Robinson and D. J. Tweet, Rep. Prog. Phys. **55**, 599 (1992).
[20] I. K. Robinson, Phys. Rev. B **33**, 3830 (1986).
[21] E. Vlieg, J. Appl. Crystallogr. **30**, 532 (1997).
[22] M. J. Buerger, *Kristallographie* (Walter de Gruyter, Berlin, 1977).
[23] R_u is defined as: $R_u=\Sigma\|F_{obs}|-|F_{calc}\|/\Sigma|F_{obs}|$, where F_{obs} and F_{calc} are the observed and calculated structure factors, respectively, and the summation runs over all datapoints.
[24] Report of the International Union of Crystallography, Subcommitee on Statistical Descriptors. Acta Crystallogr., Sect. A: Found. Crystallogr. **45**, 63 (1986).
[25] S. C. Abrahams, Acta Crystallogr., Sect. A: Cryst. Phys., Diffr., Theor. Gen. Crystallogr. **25**, 165 (1969).
[26] Edward Prince, *Mathematical Techniques in Crystallographic Computing* (Springer, Berlin, 1994).
[27] H. L. Meyerheim, R. Popescu, D. Sander, J. Kirschner, O. Robach, and S. Ferrer, Phys. Rev. B **71**, 035409 (2005).
[28] H. L. Meyerheim, V. Stepanyuk, A. L. Klavsyuk, E. Soyka, and J. Kirschner, Phys. Rev. B **72**, 113403 (2005).
[29] N. A Levanov, V. S. Stepanyuk, W. Hergert, D. I. Bazhanov, P. H.

Dederichs, A. A. Katsnelson, and C. Massobrio, Phys. Rev. B **61**, 2230 (2000).
[30] S. Fähler and H. U. Krebs, Appl. Surf. Sci. **96-98**, 1980 (1998).
[31] R. J. Behm, K. Christman, G. Ertl, M. A. Van Hove, P. A. Thiel, and W. H. Weinberg, Surf. Sci. **88**, L59 (1979).
[32] J. Quinn, Y. S. Li, D. Tian, H. Li, F. Jona, and P. M. Marcus, Phys. Rev. B **42**, 11348 (1990).
[33] J. Burchhardt, E. Lundgren, M. M. Nielsen, J. N. Andersen, and D. L. Adams, Surf. Rev. Lett. **3**, 1339 (1996).
[34] S. H. Kim, H. L. Meyerheim, J. Barthel, J. Kirschner, J. Seo, and J.-S. Kim, Phys. Rev. B **71**, 205418 (2005).
[35] S. C. Jung and M. H. Kang, Phys. Rev. B **72**, 205419 (2005).
[36] S. Wilke, D. Hennig, and R. Löber, Phys. Rev. B **50**, 2548 (1994).
[37] H. L. Meyerheim, M. Przybylski, Y. Shi, A. Ernst, J. Henk, E. Soyka, and J. Kirschner (unpublished).
[38] H. L. Meyerheim, E. Soyka, and J. Kirschner (unpublished).